

# Optimization of process parameters of pulsed TIG welded maraging steel C300

**P Deepak, M J Jualeash, J Jishnu, P Srinivasan, M Arivarasu\*, R Padmanaban and S Thirumalini**

Department of Mechanical Engineering, Amrita School of Engineering, Coimbatore, Amrita Vishwa Vidyapeetham, Amrita University, India.

**E-mail:** m\_arivarasu@cb.amrita.edu

**Abstract:** Pulsed TIG welding technology provides excellent welding performance on thin sections which helps to increase productivity, enhance weld quality, minimize weld costs, and boost operator efficiency and this has drawn the attention of the welding society. Maraging C300 steel is extensively used in defence and aerospace industry and thus its welding becomes an area of paramount importance. In pulsed TIG welding, weld quality depends on the process parameters used. In this work, Pulsed TIG bead-on-plate welding is performed on a 5mm thick maraging C300 plate at different combinations of input parameters: peak current ( $I_p$ ), base current ( $I_b$ ) and pulsing frequency (HZ) as per box behnken design with three-levels for each factor. Response surface methodology is utilized for establishing a mathematical model for predicting the weld bead depth. The effect of  $I_p$ ,  $I_b$  and HZ on the weld bead depth is investigated using the developed model. The weld bead depth is found to be affected by all the three parameters. Surface and contour plots developed from regression equation are used to optimize the processing parameters for maximizing the weld bead depth. Optimum values of  $I_p$ ,  $I_b$  and HZ are obtained as 259 A, 120 A and 8 Hz respectively. Using this optimum condition, maximum bead depth of the weld is predicted to be 4.325 mm.

**Keywords:** Pulsed TIG; Maraging C300; Mathematical model; Response Surface Methodology

## 1. Introduction

Maraging C300 steel is extensively used in aerospace and aircraft industries. They play a major role in manufacturing of aircraft landing gear, helicopter drive shafts and as armour in defence applications. Maraging steel possesses properties such as superior strength, excellent toughness, decent formability and acceptable weldability which gives the steel edge over other materials in aerospace industry [1-3]. Although possessing low carbon content, their ultrahigh strength is derived from the precipitation of intermetallic compounds such as Ni-Ti and Fe-Ni. Primary alloying element is nickel and secondary include molybdenum, cobalt and titanium. These special steels exhibit exceptional strength due to transformation of its microstructure from austenite to martensite by ageing [4-6]. Owing to overall economy and consistent weld quality, GTA welding is used in many critical applications. Out of the arc welding processes, autogenous welding can be performed using Tungsten inert gas (TIG) welding with good weld quality [7-9]. Distortion is the main concern in welding of thin plates, various researchers have reported that current pulsing shall produce welds having better penetration, reduced distortion, narrow heat affected zone and minimised residual stresses [9-12]. All these factors improve



metallurgical properties thereby enhancing mechanical properties. As reported by Balasubramanian et al. [13] current pulsing eliminates the micro segregation in the inter-dendritic region due to the reduced heat input. It is also reported that weld metal properties have been improved by usage of pulsing current [14]. As reported by many researchers, carbon migration is a prospective drawback and is extremely unenviable as it makes the material more brittle due to formation of carbides in unwanted locations. Also it results in carbon denuded soft zone thereby reducing the tensile strength. It is also reported that pulsed current has seized elemental migration (especially carbon) than continuous welds [15].

Quality of welded joints is largely affected by the welding process parameters. The quality of autogenous weld joint can be assessed by various bead geometric characteristics such as penetration, width and depth [16]. Welding is influenced by many input parameters therefore it can be considered as multi-input, multi-output process. Kumar et al. [17] has showed that optimized parameters increases the mechanical properties. For achieving the best weld quality, nowadays design of experiments (DOE) are widely applied to formulate mathematical models between welding input parameters and output variables to determine the optimal welding input parameters. The experimental optimization of any welding process is usually a highly expensive and arduous task, due to many kinds of associated non-linear events. Response Surface Methodology (RSM) serves as an alternative to this expensive experimental process. RSM is an assortment of statistical techniques used when the output (response) is affected by numerous input variables and the main aim is to optimize the response [18]. A Survey done by Benyounis et al. [19] for modelling, controlling and optimizing of various welding process unveils high level of interest in incorporation of response surface methodology (RSM) to predict response and optimize welding process. Effect of parameters on response can be studied using RSM and optimal values can be obtained using contour plots [20]. Box behnken design is adopted because it is an economical model compared to the central composite method, since it has less no of design points [21]. Important input parameters identified are pulsing frequency, background current and peak current.

There is not much work done in pulsed TIG welding of maraging C300 grade steel. A through literature review shows a considerable amount of welding is reported using filler wires and there is no significant mentioning of autogenous welding of C300. In this research work, an effort has been made to optimize the pulsed TIG welding process parameters for autogenous welding of C300 steel. Bead on trials were carried out on the C300 using the combination of parameters achieved through the response surface methodology (RSM). An attempt is made to maximise the weld penetration (response) using RSM and obtain the optimal condition for autogenous welding of C300.

## 2. Experimental Procedure

For the purpose of bead on plate welding, a C300 material of dimension 220×70×5mm was taken. Fifteen weld parameters were decided by varying the pulsing frequency and the currents (peak and base) suitable for maraging C300 steel. The chemical composition of maraging C300 is shown in table 1. Bead on plate weld was done for the following 15 parameters for a weld length of 70mm. Maraging steel is readily weldable, so no preheating was carried out during the welding. Bead-on-plate welding was done by using commercial Tungsten inert gas welding equipment (KEMPPI ARC300) in pulsed mode. A 2% thoriated tungsten electrode was used for welding with a diameter of 2.4mm. Argon gas with a flow rate of 18 lpm was used for shielding the weld pool. During welding, a constant speed of 1mm.sec<sup>-1</sup> was maintained. The plates were clamped during welding to arrest the lateral movement. Since, maraging steel is a high chromium nickel alloy stainless steel, wire brush was employed to clean between the welds. Photograph of the post bead-on-plate trial welds is shown in figure 1. After welding, the welded metal was cut in perpendicular direction of the weld in its cross section. The weld cross sections was then polished using linisher polisher followed by emery papers of four grades namely Grade300, Grade400, Grade600 and Grade 1000, finally disc polisher was

used. Then etching was done using the mixed etchant (20ml HCl, 5ml Glycerol + 0.25g CuSO<sub>4</sub> + 1ml HNO<sub>3</sub>).

**Table 1.** Composition of parent material.

Material	Element (wt. %)									
	C	Ni	Co	Mo	Ti	Al	Cr	Si	Mn	Fe
Maraging C300	0.016	18.546	8.523	4.913	0.688	0.098	0.102	0.067	0.079	Bal



**Figure 1.** Photograph showing the bead-on-plate trial welds over C300.

Weld bead depth was measured by using Carl zeiss microscope and with the help of motic software. Photographs of the macrostructures revealing bead depth is shown in table 2. Using the weld bead depth, optimization for the welding parameter on maraging steel (grade 300) was carried out using RSM. Box behnken method was used since the treatment points are the midpoints of the edges of our experimental space. It needs three continuous factors, the factors used are: pulsing frequency, base current and peak current.

Box behnken method has no axial points, thus ensuring the design points lie within the safe operating zone. Fifteen bead on trials with different combinations of pulsed current parameters were welded. The bead shape, aspect and the quality of the weld was visually inspected to find the operating range of the welding parameters.

From the analysis of the above said bead-on trials the following observations can be listed out:

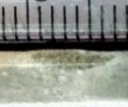
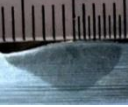

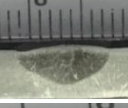

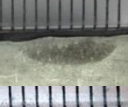
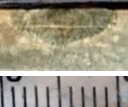

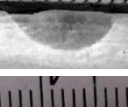
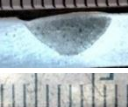



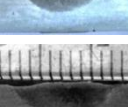
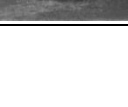
1. If the peak current ( $I_p$ ) was below 260 A, incomplete fused spots and partial weld penetration occurred, and when the current was greater than 290 A undercut and excessive spattering was seen.
2. If the base current was less than 80 A, then the arc length was short and if it was higher than 120 A arc wandering occurred.
3. If the pulsing frequency (HZ) was less than 6 Hz, the bead contour had no distinction from constant current weld beads.

Bead-on-plate pulsed TIG welded trials conducted as per box behnken design is shown in table 3. Also, weld bead depth obtained from experiments along with its predicted value and deviation from actual weld bead depth is shown in table 3.

### 3. Development of model

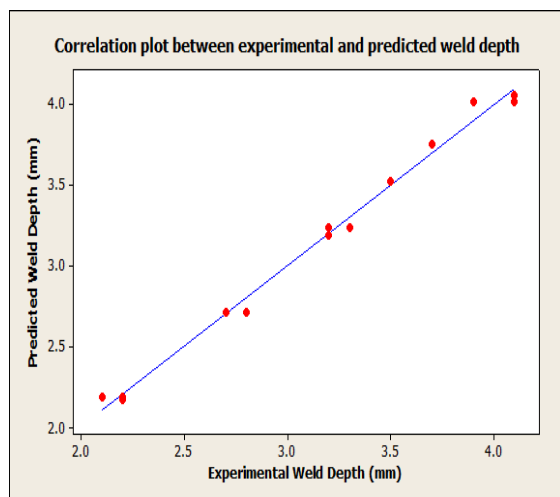
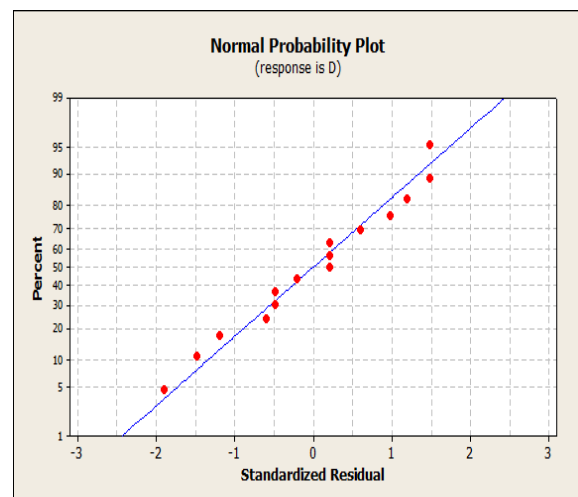
Response Surface Methodology (RSM) was utilised to establish a mathematical model for calculating the weld depth (D) of the bead-on-plate welding of maraging steel as a function of  $I_p$ ,  $I_b$  and HZ. The following second order polynomial equation (1) governs the relation between weld bead depth (D) and input parameters namely peak current ( $I_p$ ), base current ( $I_b$ ) and pulsing frequency (HZ):

**Table 2.** Macrostructure of the bead on plate welded trials showing weld depth.

Trial no.	$I_p$ (A)	$I_b$ (A)	Pulse (Hz)	Macrostructures	Bead Depth (mm)
1.	240	80	8		2.2
2.	290	80	8		3.7
3.	240	120	8		4.1
4.	290	120	8		3.5
5.	240	100	6		2.1
6.	290	100	6		2.7
7.	240	100	10		2.2
8.	290	100	10		2.8
9.	265	80	6		3.2
10.	265	120	6		4.1
11.	265	80	10		3.2
12.	265	120	10		3.9
13.	265	100	8		3.2
14.	265	100	8		3.3
15.	265	100	8		3.2

**Table 3.** Matrix of process parameters, experimental results and predicted results.

S. No.	$I_p$ (A)	$I_b$ (A)	Pulse (Hz)	Measured (D) (mm)	Predicted (D) (mm)	Error
1.	240	80	8	2.2	2.1750	0.025
2.	290	80	8	3.7	3.7500	-0.05
3.	240	120	8	4.1	4.0500	0.05
4.	290	120	8	3.5	3.5250	-0.025
5.	240	100	6	2.1	2.1875	-0.0875
6.	290	100	6	2.7	2.7125	-0.0125
7.	240	100	10	2.2	2.1875	0.0125
8.	290	100	10	2.8	2.7125	0.0875
9.	265	80	6	3.2	3.1875	0.0125
10.	265	120	6	4.1	4.0125	0.0875
11.	265	80	10	3.2	3.1875	0.0125
12.	265	120	10	3.9	4.0125	-0.1125
13.	265	100	8	3.2	3.2333	-0.03333
14.	265	100	8	3.3	3.2333	0.06667
15.	265	100	8	3.2	3.2333	-0.03333

**Figure 2.** Correlation plot between experimental and predicted weld bead depth.**Figure 3.** Normal probability plot of residuals.

$$D = b_0 + b_1 I_p + b_2 I_b + b_3 HZ + b_{11} I_p^2 + b_{22} I_b^2 + b_{33} HZ^2 + b_{12} I_p I_b + b_{23} I_b HZ + b_{13} I_p HZ \quad (1)$$

Where,  $b_0$  is the average of responses and  $b_1, b_2, b_{11}, b_{22}, \dots, b_{13}$  depend on the main and interaction effects of the input parameters. Raymond H.M [22] has explained about Response Surface Methodology and details regarding experimental designs and formulation of regression equation can be found in it. Minitab software package was used to obtain the above mentioned coefficients. The significance of the coefficients was assessed and tested at 95% confidence level.

Significant coefficients were discerned and were included in the final model for calculating the weld bead depth as given below (equation (2)):

$$D = -74.4057 + 0.543033 I_p - 0.0240417 I_b + 1.11667 HZ - (8.06667 E^{-04} I_p^2) + 0.00161458 I_b^2 - 0.0697917 HZ^2 - 0.00105 I_p I_b \quad (2)$$

ANOVA was used to evaluate the acceptability of the developed model and the results are shown in table 4. For a term to be significant in the formulated model, its probability value (P) should be less than 5%. The P values for linear and quadratic terms were found out to be very small (less than 0.001). Although P value for linear term HZ was 1.000 ( $>0.05$ ) and is therefore insignificant, was included in the model because its quadratic term had significant effects. Interaction terms  $I_p \times HZ$  and  $I_b \times HZ$  are not significant as they have P values 1.000 and 0.310 (both greater than 0.05). So the above interaction terms are eliminated from the model and run again to get the values as shown in table 4. The Lack-of-fit value is greater than 0.05 (P value: 0.305), implying that formulated quadratic model is adequate. The coefficient of determination ( $R^2=0.9919$ ) denotes that only less than 1% of the overall variations is not accounted by the model. The coefficients  $R^2_{pred}$  (0.9571) and  $R^2_{adj}$  (0.9838) also strongly suggests that the insignificant terms were excluded from the model.

As shown in figure 2, the measured and predicted weld depth values have a close interrelationship. The data points come close to each other almost making a straight line indicating the linear relationship shared by the two variables. The normal probability plot of residuals is depicted in figure 3. In the plot we can see that the residuals of weld depth lie on a straight line. We can therefore infer that the error while comparing the measured values and predicted values are normally distributed. The developed model is highly apposite since the errors obtained are distributed normally and P value of lack-of-fit is 0.305 ( $>0.05$ ), making it insignificant.

**Table 4.** ANOVA results showing acceptability of the model.

Source	DF	Sum of Squares	Mean Squares	F	P
Regression	7	6.00683	0.85812	122.17	0.000
Linear	3	1.91250	0.63750	90.76	0.000
Square	3	2.99183	0.99728	141.99	0.000
Interaction	1	1.10250	1.10250	156.97	0.000
Residual Error	7	0.04917	0.00702		
Lack-of-fit	5	0.04250	0.00850	2.55	0.305
Pure error	2	0.00667	0.00333		
Total	14	6.05600			

$$SD = 0.0838082, \text{ Press} = 0.26, R^2 = 99.19\%, R^2_{pred} = 95.71\%, R^2_{Adj} = 98.38\%$$

#### 4. Results and Discussion

Bead-on-plate pulsed TIG welding of maraging C300 was successfully completed at  $I_p$ ,  $I_b$  and HZ ranging from 240 A to 290 A, 80 A to 120 A and 6 Hz to 10 Hz respectively. RSM was incorporated to develop the model for weld depth of the joints. The formulated model was utilised to study the effect of  $I_p$ ,  $I_b$  and HZ on the weld depth of the joints and to reach the optimum condition for maximum depth. Further the results are depicted graphically in figures 4-6.

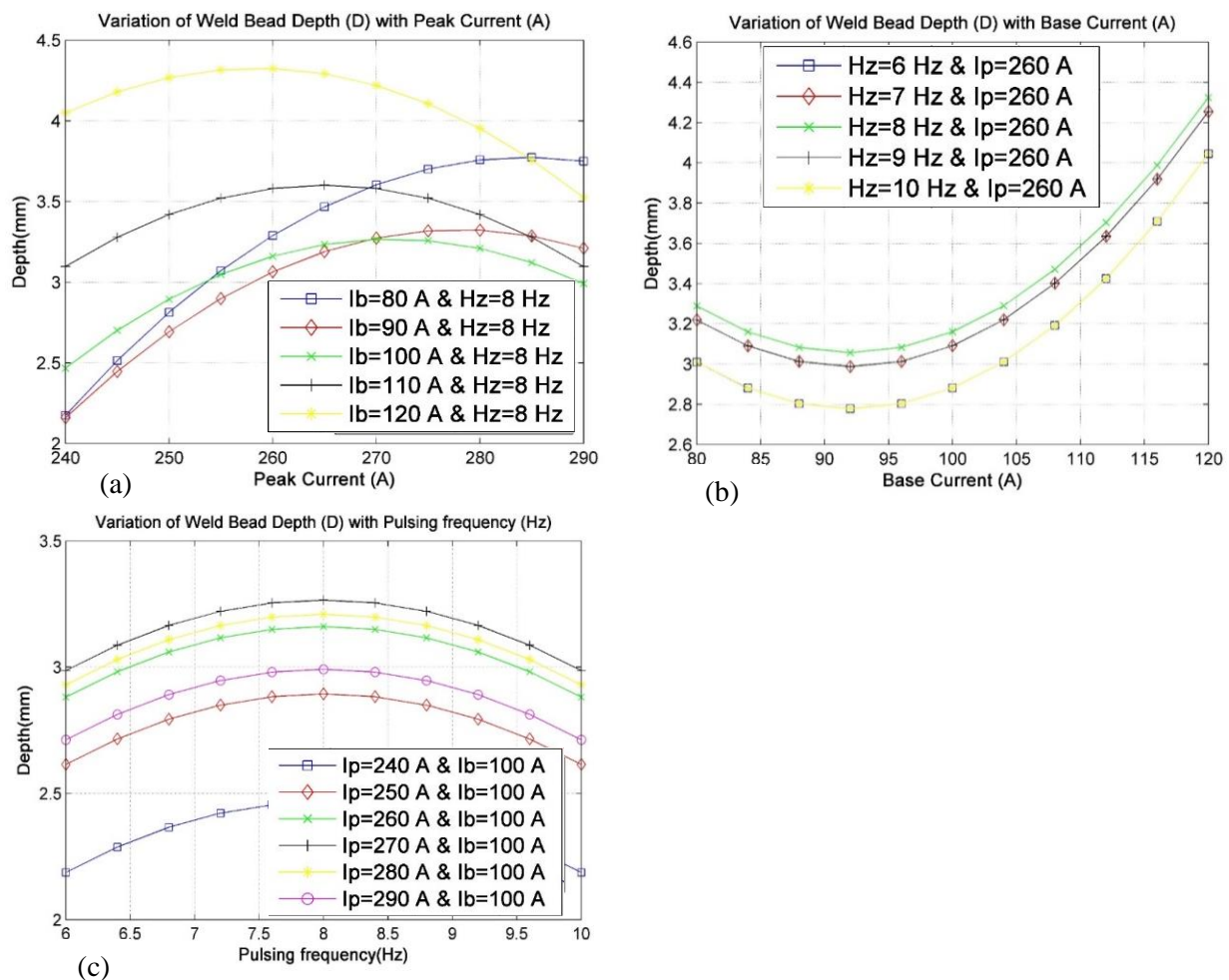
##### 4.1. Effect of Peak current

Variation of weld bead depth (D) with respect to Peak current ( $I_p$ ) at a constant pulsing frequency, suitably with the central value 8 Hz is plotted and shown in figure 4(a). From the figure, we observed that by increasing  $I_p$  from 240 A to 290 A, weld bead depth first increased then started to drop after

reaching a maximum point for all values of base current ( $I_b$ ). The pattern of variation of weld bead depth remained the same irrespective of  $I_b$ . Also weld bead made at an  $I_p$  around 260A to 280A yielded the maximum weld depth for a given  $I_b$ . Maximum weld depth was obtained when  $I_b=120$  A and minimum was obtained at  $I_b=80$  A.

#### 4.2. Effect of Base current

The effect of base current ( $I_b$ ) on the weld depth of the pulsed TIG welded maraging C300 plate is shown in figure 4(b). The plot was made at a constant  $I_p$  value of 260 A. It was noted that when  $I_b$  was increased till 95 A, there was a decrease in weld depth. Further increase in  $I_b$  till 120 A resulted in an increase in the weld depth. The pattern of variation remained the same irrespective of pulsing frequency. For any pulsing frequency, weld depth was found to be maximum at  $I_b=120$  A. Also maximum weld depth was obtained at pulsing frequency of 8 Hz and minimum at 10 Hz.



**Figure 4.** Line plot showing the variation of weld bead depth with respect to input parameters.

#### 4.3. Effect of Pulsing frequency

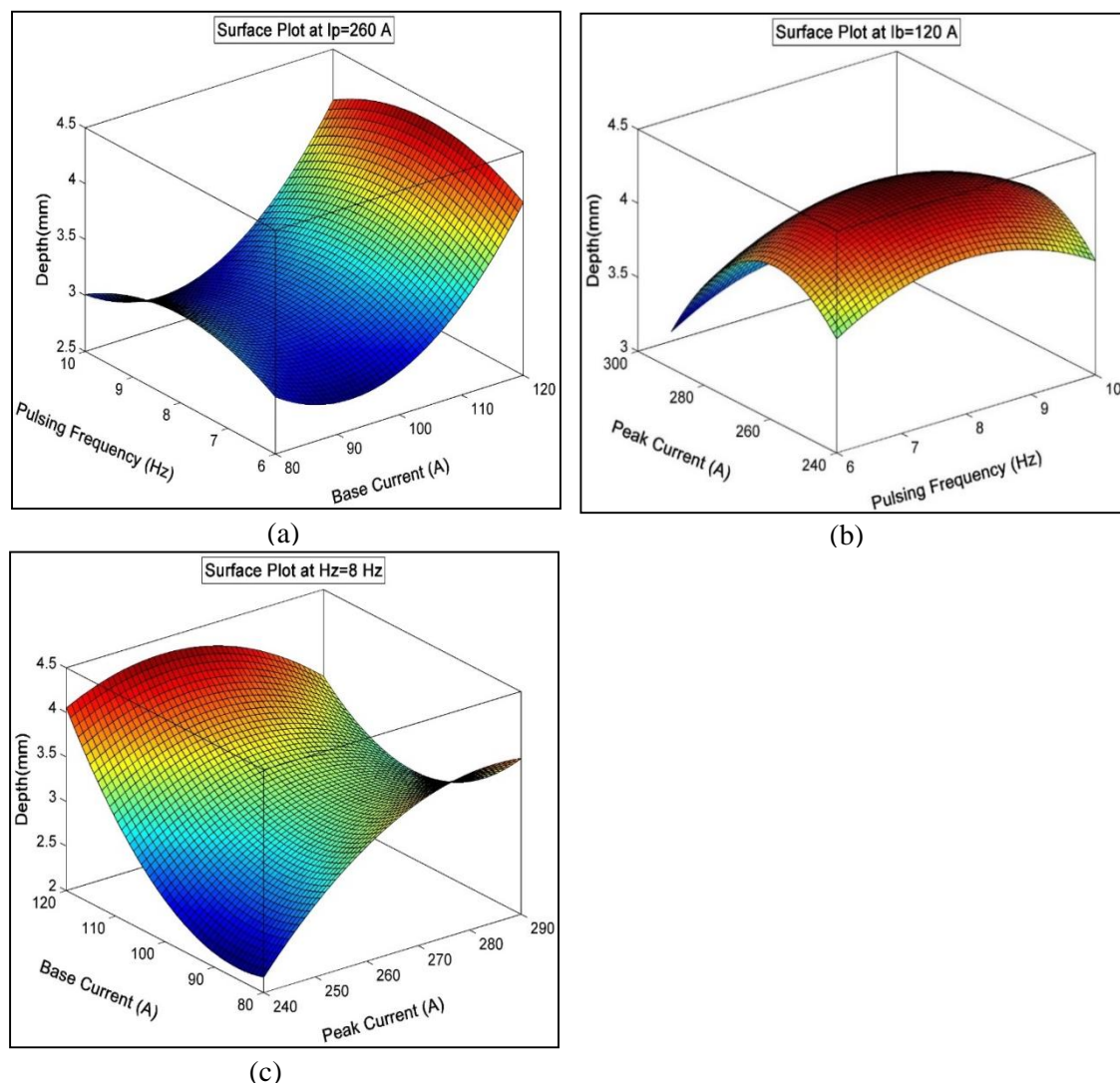
Variation of weld bead depth (D) with pulsing frequency (HZ) is shown in figure 4(c). Similar trend to that of peak current was observed. The plot was made at a constant base current ( $I_b$ ) of 100 A. From figure 4(c), we observed that varying pulsing frequency from 6 Hz to 8 Hz caused the weld depth to increase. Further increase in pulsing frequency till 10 Hz resulted in a decrease in weld depth. The

trend remained same irrespective of peak current used. Maximum depth was obtained when  $I_p=270$  A and minimum at  $I_p=240$  A.

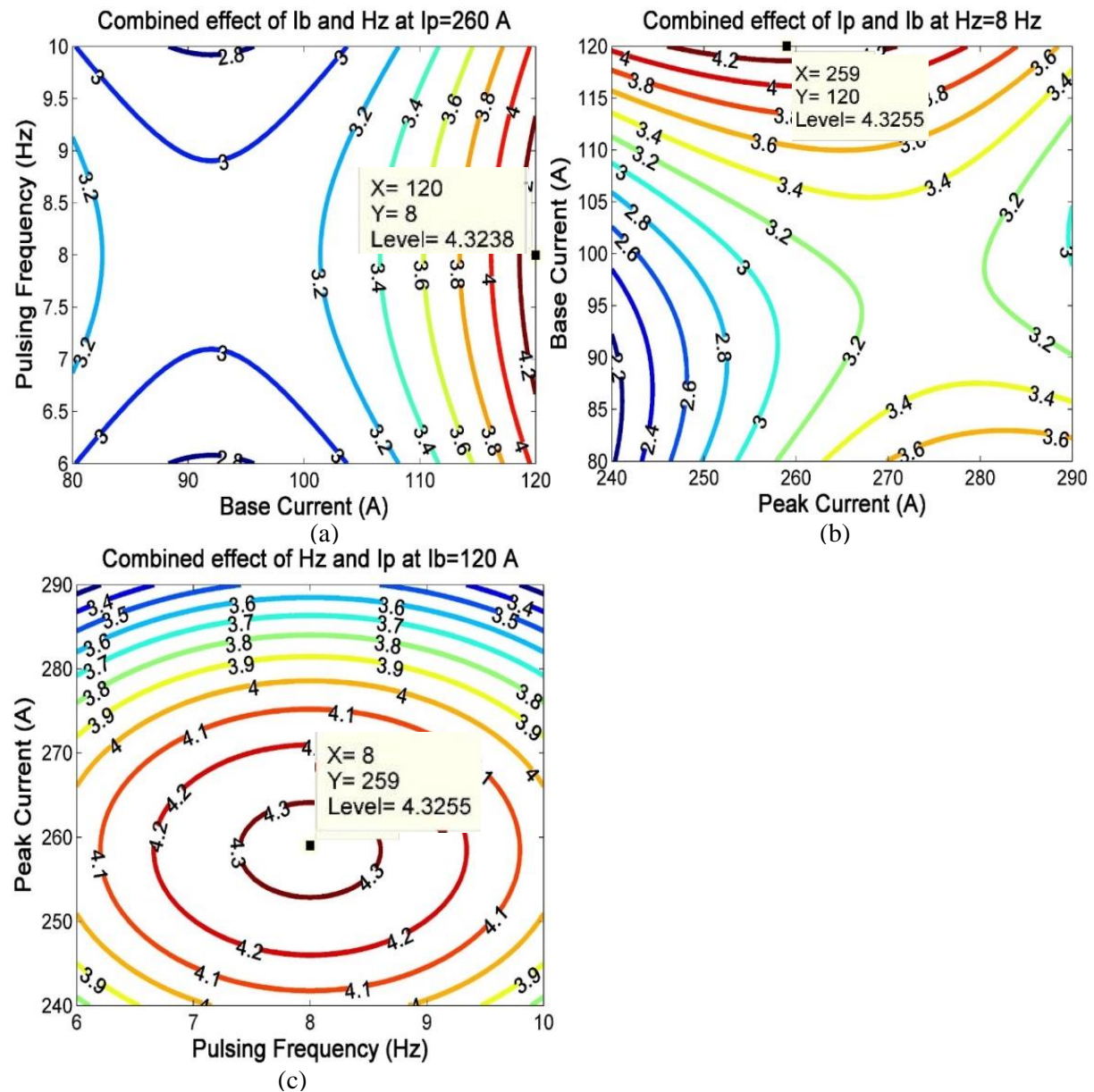
**Table 5.** Optimized input parameters obtained.

Optimum conditions			Predicted weld bead depth (mm)
Peak current (A)	Base current (A)	Pulsing frequency (Hz)	
259	120	8	4.325

The surface plot showing the variation of weld bead depth (D) with different combinations of  $I_p$ ,  $I_b$  and HZ is shown in figure 5. It was observed that for a base current of  $I_b=120$  A, maximum weld depth was obtained as compared to a constant central value of  $I_b=100$  A which produced less depth. For the process of optimization (maximizing weld depth),  $I_b=120$  A was taken into consideration for plotting figure 5(b). The surface plots revealed that maximum weld bead depth was obtained when peak current ( $I_p$ ) was between 255 A to 270 A, base current ( $I_b$ ) was around 118 A to 120 A and pulsing frequency (HZ) was between 7.5 Hz to 8.5 Hz.



**Figure 5.** Surface plot at constant Peak current, base current and pulsing frequency.



**Figure 6.** Contour plot at constant peak current, base current and pulsing frequency.

The contour plot of weld bead depth at different combinations of  $I_p$ ,  $I_b$  and  $HZ$  is depicted in figure 6. It was observed from the contour plots that maximum weld bead depth was obtained when the peak current, base current and pulsing frequency were respectively 259 A, 120 A and 8 Hz. Corresponding average weld bead depth was obtained as 4.325 mm. Hence, the optimized input parameter setting for maximum weld depth is found out and shown in table 5.

## 5. Conclusion

Bead-on-plate pulsed TIG welding trials were performed on maraging C300 under varying values of Peak current ( $I_p$ ), base current ( $I_b$ ) and pulsing frequency (HZ) and the weld bead depth was measured. The Response Surface Methodology (RSM) was used to develop a mathematical model (regression) of weld bead depth (D) in terms of  $I_p$ ,  $I_b$  and  $HZ$ . The regression model was used to investigate the effect of  $I_p$ ,  $I_b$  and  $HZ$  on the weld bead depth. Using various plots developed from regression equation, the optimum condition was arrived. The following conclusions were made from the investigation:

1. The weld bead depth was found to depend on peak current, base current and pulsing frequency.
2. At a constant HZ; increasing  $I_p$  from 240 A to 290 A, weld bead depth first increased then started to drop after reaching a maximum point for all values of  $I_b$ .
3. At a constant  $I_p$ ; increase in  $I_b$  till 95 A caused decrease in weld depth. Further increase in  $I_b$  till 120 A resulted in an increase in the weld depth for all values of HZ.
4. At a constant  $I_b$ ; varying HZ from 6 Hz to 8 Hz caused the weld depth to increase. Further increase in HZ till 10 Hz resulted in a decrease in weld depth for all values of  $I_p$ .
5. The optimum parameters for achieving maximum weld bead depth (maximum penetration) in autogenous pulsed TIG welding of maraging C300 are found to be, Peak current ( $I_p$ ): 259 A, Base current ( $I_b$ ): 120 A and Pulsing frequency (HZ): 8 Hz.

## References

- [1] Shamantha CR, Narayanan R et al 2000. *Mater. SciEng. A* **287** 43–51.
- [2] Poinke LJ, Garland KC 1973 Evaluation of shuttle solid rocket booster case materials. Technical Report, NASA.
- [3] Harold Whitfield K 2003 Solid rocket motor metal cases, case file copy NASA April 1970.
- [4] Degarmo, E Paul, Black, J T Kohser, Ronald A *Materials and Processes in Manufacturing* (9th ed.), Wiley, p. 119, **ISBN 0-471-65653-4**
- [5] Subhananda Rao G, Venkata Rao B, Nageswara Rao 2005. *Eng Fail Anal* **12** 325–36.
- [6] Fawad Tariq, Rasheed Ahme6d Baloch, Bilal Ahmed NausheenNaz 2010 *J Mater Eng Perform* **19** 264–73.
- [7] Nagarajan KV 1998 Welding aspects of maraging steels In: Proceedings of the conference on steels for engineering industries-trends in weldability, Indian Institute of Metals, Tiruchirapalli, India. p. 43–53.
- [8] Cary HB 1989 Modern welding technology NJ: Prentice-Hall
- [9] Kou S, Le Y 1986 Nucleation mechanism and grain refining of weld metal *Weld J* **65**(4) 65–70
- [10] Arivarasu M, Devendranath R K, Arivazhagan N 2015 . *Materials Research* **18** 59-77.
- [11] Tseng CF, Savage WF 1971 *weld J* **50**(11) 777–86.
- [12] Madusudhan Reddy G, Gokhale AA, Prasad Rao K 1997 *J Mater Sci* **32** 4117–21.
- [13] Balasubramanian V, Ravishankar V, Madhusudhan Reddy G 2008 *Int. J. Adv.Manuf.Technol.* **36** 254–62
- [14] Balasubramanian V, Jayabalan V, Balasubramanian M 2008 *Materials and Design* **29** 1459–1466.
- [15] Vijay, Ukadgaonker G, Bhat Sunil, Jha 2008 *Int J Fatigue* **30** 689–705 reference guide.
- [16] DaviSampaioCorreia, CristieneVasconcelosGonçalves, et al 2005 *J. Mater. Proc. Technol.* **160** 70–76.
- [17] Kumar A, Sundarajan S 2009 *Materials and Design* **30** 1288–1297.
- [18] DenizBaş, İsmail H Boyacı 2007 *Journal of Food Engineering* Volume **78**, Issue 3, Pages 836–84.
- [19] Benyounis KY, Olabi AG *A Advances in Engineering Software* **39** 483–496.
- [20] Padmanaban R, Balusamy V, Nouranga KN 2015 *Journal of Engineering Science and Technology* Vol. **10**, No. 6 790 – 801.
- [21] Ferreira SLC, Bruns RE et al 2007 Box-Behnken design: *AnalyticaChimicaActa*. Volume **597**, Issue 2, Pages 179–186.
- [22] Raymond HM, Douglas CM and Christine MAC 2001 (3rded.) John Wiley & Sons Inc.